Ferucarbotran-Enhanced Hepatic MRI at 3T Unit: Quantitative and Qualitative Comparison of Fast Breath-hold Imaging Sequences

Kyung Eun Cho, Jeong-Sik Yu, Jae-Joon Chung, Joo Hee Kim, Ki Whang Kim

Purpose : To compare the relative values of various fast breath-hold imaging sequences for superparamagnetic iron-oxide (SPIO)-enhanced hepatic MRI for the assessment of solid focal lesions with a 3T MRI unit.

Materials and Methods : 102 consecutive patients with one or more solid malignant hepatic lesions were evaluated by spoiled gradient echo (GRE) sequences with three different echo times (2.4 msec [GRE_2.4], 5.8 msec [GRE_5.8], and 10 msec [GRE_10]) for T2*-weighted imaging in addition to T2-weighted turbo spin echo (TSE) sequence following intravenous SPIO injection. Image qualities of the hepatic contour, vascular landmarks and artifacts were rated by two independent readers using a four-point scale. For quantitative analysis, contrast-to-noise ratio (CNR) was measured in 170 solid focal lesions larger than 1 cm (107 hepatocellular carcinomas, nine cholangiocarcinomas and 54 metastases).

Results : GRE_5.8 showed the highest mean points for hepatic contour, vascular anatomy and imaging artifact presence among all of the subjected sequences ($p < 0.001$) and was comparable ($p = 0.414$) with GRE_10 with regard to lesion conspicuity. The mean CNRs were significantly higher ($p < 0.001$) in the following order: GRE_10 (24.4±14.5), GRE_5.8 (14.8±9.4), TSE (9.7±6.3), and GRE_2.4 (7.9 ±6.4). The mean CNRs of CCCs and metastases were higher than those of HCCs for all imaging sequences ($p < 0.05$).

Conclusion : Regarding overall performances, GRE using a moderate echo time of 5.8 msec can provide the most reliable data among the various fast breath-hold SPIO-enhanced hepatic MRI sequences at 3T unit despite the lower CNR of GRE_5.8 compared to that of GRE_10.

Index words : Liver neoplasm
Magnetic resonance (MR)
Superparamagnetic iron oxide (SPIO)

JKSMRM 14:31-40(2010)

[1]Department of Radiology and Institute of Radiological Science, Yonsei University College of Medicine, Gangnam Severance Hospital, Seoul, Korea

Received; February 22, 2010, revised; May 13, 2010, accepted; May 25, 2010

Corresponding author : Jeong-Sik Yu, M.D., Department of Radiology, Yonsei University College of Medicine, Gangnam Severance Hospital, 712 Eonjuro, Gangnam-gu, Seoul 135-720, Korea.
Tel. 82-2-2019-3510 Fax. 82-2-3462-5472 E-mail: yjsrad97@yuhs.ac

Introduction

In addition to the non-specific extracellular contrast agents used in dynamic imaging, a variety of liver-specific contrast agents have been used to assess focal liver lesions (1). The primary role of the superparamagnetic iron oxide (SPIO) agent, which is taken up by Kupffer cells, is to improve the detectability of small lesions by increasing the lesion-to-liver contrast (1, 2). Many facilities now use high-field magnets for body imaging, and liver MRIs using 3T unit have become more generalized (3, 4). Compared to the more popular and standardized 1.5T unit, high-field unit such as the 3T MRI produce higher-resolution imaging due to their inherently higher signal-to-noise ratio (SNR); however, the increased instance of artifacts produced by high-field units is a potential drawback that can disturb imaging quality (especially in abdominal imaging) (3–5).

Most investigators who use 3T unit for hepatic MR imaging follow the same parameters as those that are used for 1.5T unit because optimal parameters have not been specialized to the high-field magnets in SPIO-enhanced imaging as well as in static and dynamic imaging of the liver (4, 6, 7). Potential challenges for better imaging quality include some changes in tissue-specific relaxation times, precession frequencies and susceptibility-related artifacts. The varied image quality following SPIO injection with 3T unit shows different consequences than that with 1.5T unit (3, 4, 6, 8). Like the prior studies for fast imaging sequences for SPIO-enhanced imaging in the 1.5T unit (9, 10), determination of echo time (TE) is also essential to get optimized T2*-weighted gradient echo images for the detection of small focal hepatic lesions in the 3T unit. For this purpose, image quality in terms of the anatomic details, lesion conspicuity and imaging artifact should be balanced with the high contrast between the lesion and the background parenchyma after SPIO injection (7, 10). The purpose of this study was to evaluate the relative abilities of various fast breath-hold imaging sequences for SPIO-enhanced hepatic MRI for the assessment of clinically challenging solid malignant focal lesions using a 3T unit.

Materials and Methods

Patients

Approval for this retrospective study was obtained from our institutional review board, which waived the requirement of informed consent for the review of images. We reviewed the electronic medical records of all patients who underwent hepatic MR imaging with a 3T MRI unit during a 19-month period from July 2005 to December 2006. We identified 102 consecutive patients (74 men and 28 women ranging from 22 to 81 years of age [mean, 55.2]) with one or more solid malignant focal lesions verified either by histopathologic findings or on follow-up imaging modalities other than MRI, including digital subtraction angiography, computed tomography (CT) and ultrasonography, conducted 3–12 months later, as well as with increased levels of serum tumor markers. In patients with multiple lesions, a maximum of five lesions of each type per patient were selected on the basis of the aforementioned criteria; 170 total lesions ($\geq$ 1 cm in the longest dimension) in 102 patients were selected for further analysis. We excluded lesions less than 1.0 cm in length to avoid any inaccuracies in signal intensity measurement for quantitative analysis that could result from the partial volume averaging effect in smaller lesions. Among the 170 lesions, we identified 107 hepatocellular carcinomas (HCCs) in 70 patients, 54 metastases in 27 patients and nine cholangiocarcinomas (CCCs) in five patients. For 26 HCCs, three CCCs and 41 metastases, histopathologic verification of the lesions by means of biopsy and/or surgery was possible. The primary sites of the metastatic lesions included colorectal carcinoma (33 lesions in 18 patients), gastrointestinal stromal tumor (five lesions in one patient), nasopharyngeal carcinoma (five lesions in one patient), renal cell carcinoma (four lesions in one patient), breast carcinoma (two lesions in two patients), cervical cancer (two lesions in one patient), pancreatic carcinoma (one lesion in one patient), common bile duct cancer (one lesion in one patient), and thyroid cancer (one lesion in one patient).

MRI Techniques

MR imaging was performed with a 3T unit (Signa EXCITE; GE Medical Systems, Milwaukee, WI, USA).

Patients were positioned supine with anterior and posterior phased-array coils centered over the liver. After obtaining localizer images, chemical selective fat-suppressed T2-weighted turbo spin-echo images (TR/TE, 4000/98 msec; echo train length, 14) were obtained in the axial plane. After obtaining a double-echo chemical shift gradient-echo sequence (TR/first-echo TE, second-echo TE, 160/2.4 [in-phase], 5.8 [opposed-phase]; flip angle, 70°; matrix, 352 × 300; slice thickness, 8 mm; interslice gap, 1.5 mm), dynamic contrast-enhanced imaging was obtained using a 3D gradient echo (GRE) sequence (LAVA; GE Medical Systems) with ultrafast image reconstruction using parallel imaging algorithms (ASSET factor, 2) in the axial plane (TR/TE, 3.5–4.2/1.0–1.2 msec; flip angle, 10°; matrix, 320 × 256; slice thickness, 5 mm; slice spacing, 2.5 mm; number of slices, 64) during a 16-sec breath-holding period. A dynamic series consisted of one precontrast series followed by three postcontrast series, including arterial, portal and five-minute delayed phase imaging. The postcontrast series were performed after administrating a bolus injection of gadopentetate dimeglumine (0.1 mmol/kg of Magnevist; Schering, Berlin, Germany) at a rate of 2 mL/sec followed by a saline flush using a power injector.

After the dynamic imaging, SPIO (8 μmol iron/kg of Resovist; Schering, Berlin, Germany) was intravenously administrated as the second contrast agent. After ten minutes, T2-weighted turbo spin-echo (TSE) and T1-weighted double echo chemical shift gradient-echo (GRE) images were obtained using the same parameters as those of the pre-contrast imaging. A GRE sequence with a longer echo time (TR/TE, 134/10 msec; flip angle, 35°) was added for T2*-weighted imaging. All scans were sent to the Picture Archiving and Communication System (PACS) for interpretation on PACS workstations.

Image Analysis

For all patients, three GRE sequences, including the two sequences of double echo techniques (TE, 2.4 msec [GRE_2.4]; 5.8 msec [GRE_5.8]) and another GRE using a longer TE of 10 msec for T2*-weighted imaging [GRE_10], were subjected to comparative analyses of SPIO-enhanced images, along with one fat-suppressed T2-weighted TSE sequence. The images were analyzed independently by one attending radiologist with 14 years of experience with hepatic MRIs and also by a senior resident in the department of radiology on a workstation (Centricity, GE Healthcare) using standard software. After finishing the review session, evaluation disagreements were resolved by consensus.

Qualitative image analysis was performed to identify the sharpness of hepatic contours, the visibility of intrahepatic vasculature and the presence of artifacts. To ensure rating consistency, the two readers had been previously trained in the rating of participants. The observers recorded the hepatic contours and vascular landmarks in each image set based on the following four-point scale for both the right and left lobes of the liver: 1, not visualized; 2, poorly visualized; 3, definitely visualized; 4, sharply visualized. We assessed the artifacts, including motion, vascular pulsation, chemical shift, and susceptibility artifacts, on a four-point scale using the following scores: 1, severe; 2, moderate; 3, mild; 4, absent. For all 170 lesions, the conspicuity of each lesion on each image set was also

Table 1. Qualitative Assessment Based on Image Degradation Due to Artifacts

MRI pulse sequence	Hepatic Contour		Vascular Landmark		Artifact		Lesion Conspicuity	
	Rank[a]	Mean[b]	Rank[a]	Mean[b]	Rank[a]	Mean[b]	Rank[a]	Mean[b]
TSE	4	2.67	4	1.90	4	2.46	4	2.65
GRE_2.4	2	3.47	2	3.65	2	3.65	3	2.74
GRE_5.8	1	3.65	1	3.79	1	3.68	1	3.30
GRE_10	3	3.12	3	3.16	3	2.73	2	3.09

[a] Data indicate the rank order of image quality.
[b] Data are based on reader's score of degree of image degradation (1 = severe, 2 = moderate, 3 = mild, 4 = absent).
TSE : turbo spin echo
GRE_2.4 : gradient echo with TE of 2.4 msec
GRE_5.8 : gradient echo with TE of 5.8 msec
GRE_10 : gradient echo with TE of 10 msec

evaluated based on a four-point rating scale. A score of 1 indicated that the lesion was invisible; 2, poorly defined; 3, fairly defined; 4, clearly defined. For quantitative analysis, the contrast-to-noise ratio (CNR) of each lesion was calculated using a spherical or oval region of interest (ROI) measurement by the same reviewers in conference using the following equation:

$$CNR = (SI_{lesion} - SI_{liver}) / SD_{noise},$$

Where SI_{lesion} is the signal intensity of the lesion; SI_{liver} is the signal intensity of the liver parenchyma; and SD_{noise} is the standard deviation of the background noise.

The statistical significances of the qualitative data for the four pulse sequences were determined with using Wilcoxon's matched-pair signed rank test for multiple comparisons. T-test was used to compare lesion-to-liver CNRs between the HCCs and the other solid lesions in the images with the four different pulse sequences. A p-value of less than 0.05 was considered statistically significant.

Results

On the four-point scales, the mean scores of

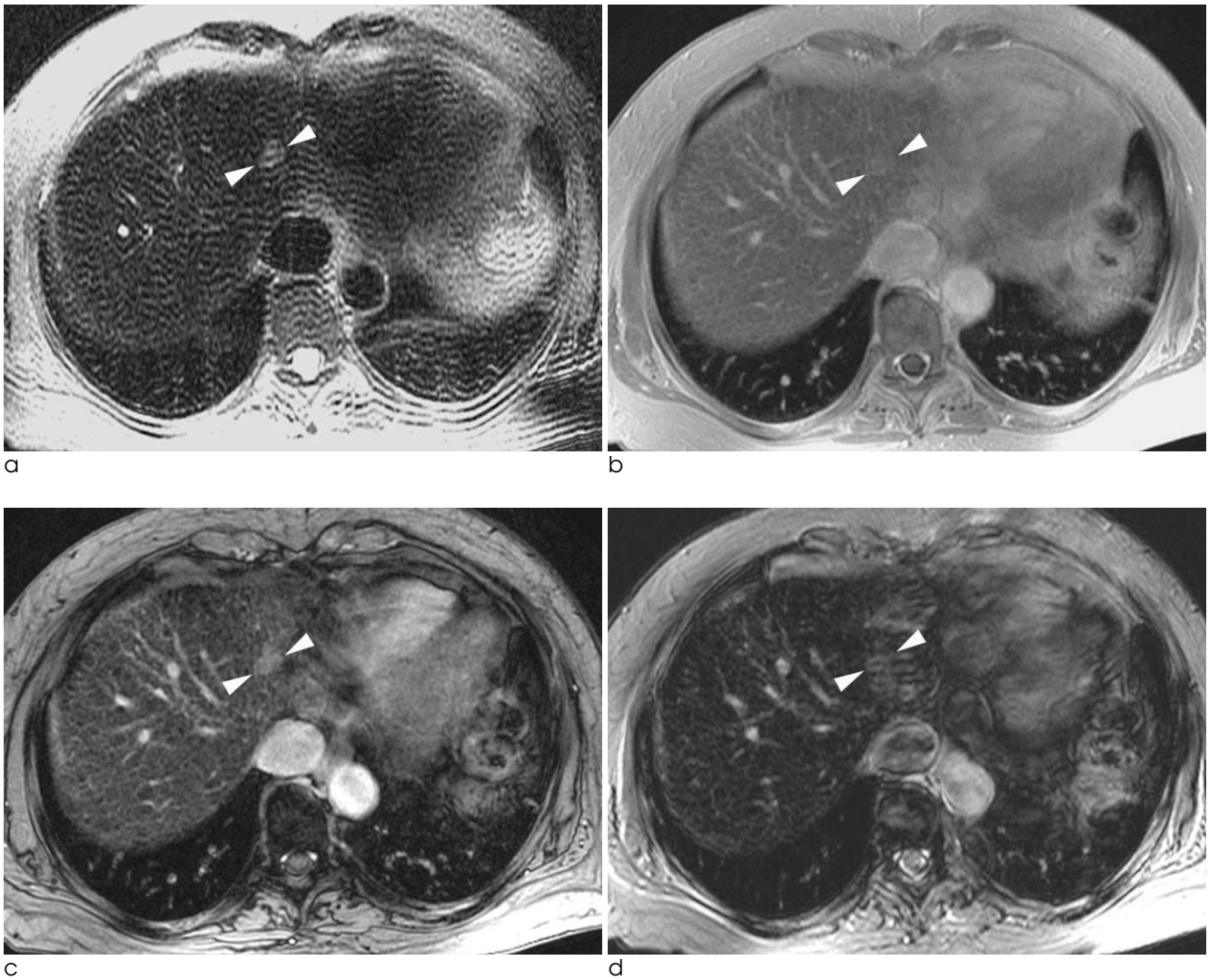

Fig. 1. A 59-year-old woman with a hepatocellular carcinoma in the cirrhotic liver. Among the four difference MRI sequences of fast imaging after ferucarbotran injection, turbo spin-echo image (a) shows worst quality in hepatic contour, vascular landmark and overall imaging artifact compared to gradient echo images using a TE of 2.4 msec (b) or 5.8 msec (c). Due to the serious pulsation artifact, the small hepatocellular carcinoma (arrowheads) in left lobe of the liver is not well defined on gradient echo imaging using a TE of 10 msec (d).

Table 2. Qualitative Assessment of Lesion Conspicuity

Lesion Conspicuity on Four Different MRI Sequences	HCCs	CCCs and Metastases	Overall
GRE_5.8 vs GRE_10	< (p = 0.696)	< (p = 0.305)	< (p = 0.386)
GRE_5.8 vs GRE_2.4	> *	> *	> *
GRE_5.8 vs TSE	> *	> (p = 0.795)	> *
GRE_10 vs GRE_2.4	> *	> *	> *
GRE_10 vs TSE	> *	> (p = 0.380)	> *
GRE_2.4 vs TSE	< *	< *	< *

* Indicate the statistically significant difference ($p < 0.05$) between two MRI sequences.
p Values for Comparison of the lesion conspicuity between each sequence in lesions with and without uptake of Superparamagnetic Iron Oxide (SPIO).
TSE : turbo spin echo
GRE_2.4 : gradient echo with TE of 2.4 msec
GRE_5.8 : gradient echo with TE of 5.8 msec
GRE_10 : gradient echo with TE of 10 msec

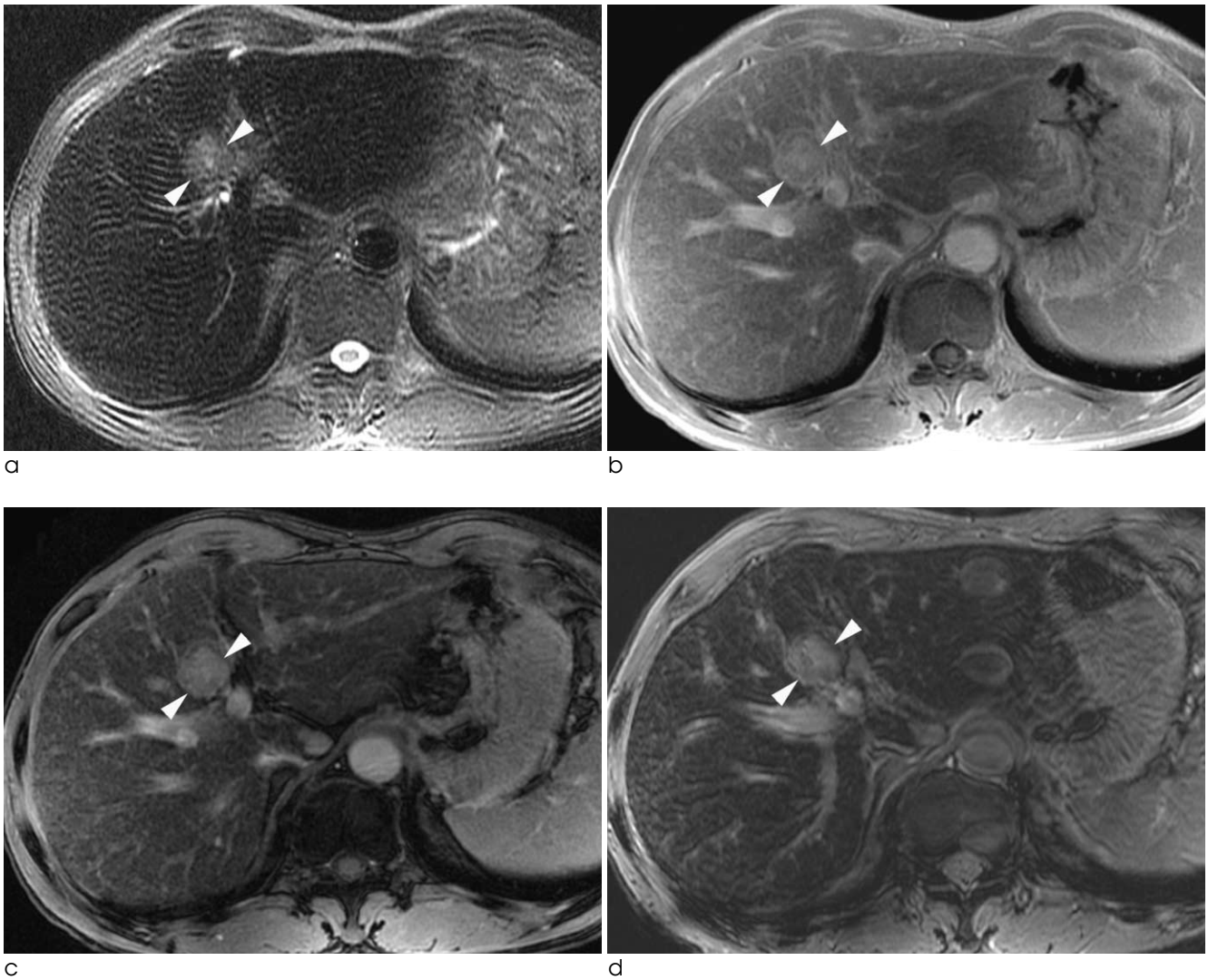

Fig. 2. A 51-year-old man with a hepatocellular carcinoma in segment 4 of the cirrhotic liver. After ferucarbotran injection, compared to turbo spin-echo image (a) or gradient echo image with a TE of 2.4 msec (b), gradient echo image with a TE of 5.8 msec (c) and gradient echo image with a TE of 10 msec (d) show better lesion (arrowheads) conspicuity.

sharpness of hepatic contours, visibility of intrahepatic vessels, presence of artifacts, and lesion conspicuity for the four sequences are shown in Table 1. Regarding the sharpness of hepatic contours, the visibility of intrahepatic vessels, or the imaging artifacts, GRE_5.8 was significantly better than GRE_2.4 ($p < 0.001$), GRE_10 ($p < 0.001$) or TSE ($p < 0.001$) (Fig. 1).

Overall lesion conspicuities of the GRE_5.8 and GRE_10 were better than those of TSE and GRE_2.4 ($p < 0.001$). For HCCs, lesion conspicuity was best on the GRE_10 but was comparable with that of GRE_5.8 without statistical significance ($p = 0.696$). GRE_5.8 and GRE_10 were superior to the other two sequences with regard to lesion conspicuity for HCCs ($p < 0.001$) (Fig. 2). For CCCs and metastases, GRE_5.8 and GRE_10 as well as TSE were superior to GRE_2.4 ($p < 0.001$) (Fig. 3, Table 2). Although the lesion conspicuity for CCCs and metastases on GRE_5.8 and GRE_10 were generally superior to those of TSE, there was no statistically significant difference between the two (GRE_5.8 vs GRE_10, $p = 0.795$; GRE_10 vs. TSE, $p = 0.380$) (Table 2).

For all lesions, the mean lesion-to-liver CNR was highest at GRE_10 (mean $\pm$ SD = 19.8 $\pm$ 14.4) and was significantly higher ($p < 0.001$) than those at GRE_5.8 (12.1$\pm$9.1), GRE_2.4 (6.3$\pm$6.4) or TSE (10.1 $\pm$7.7) (Table 3, Fig. 4). The CNRs at GRE_5.8 and TSE were comparable ($p = 0.022$) and were significantly

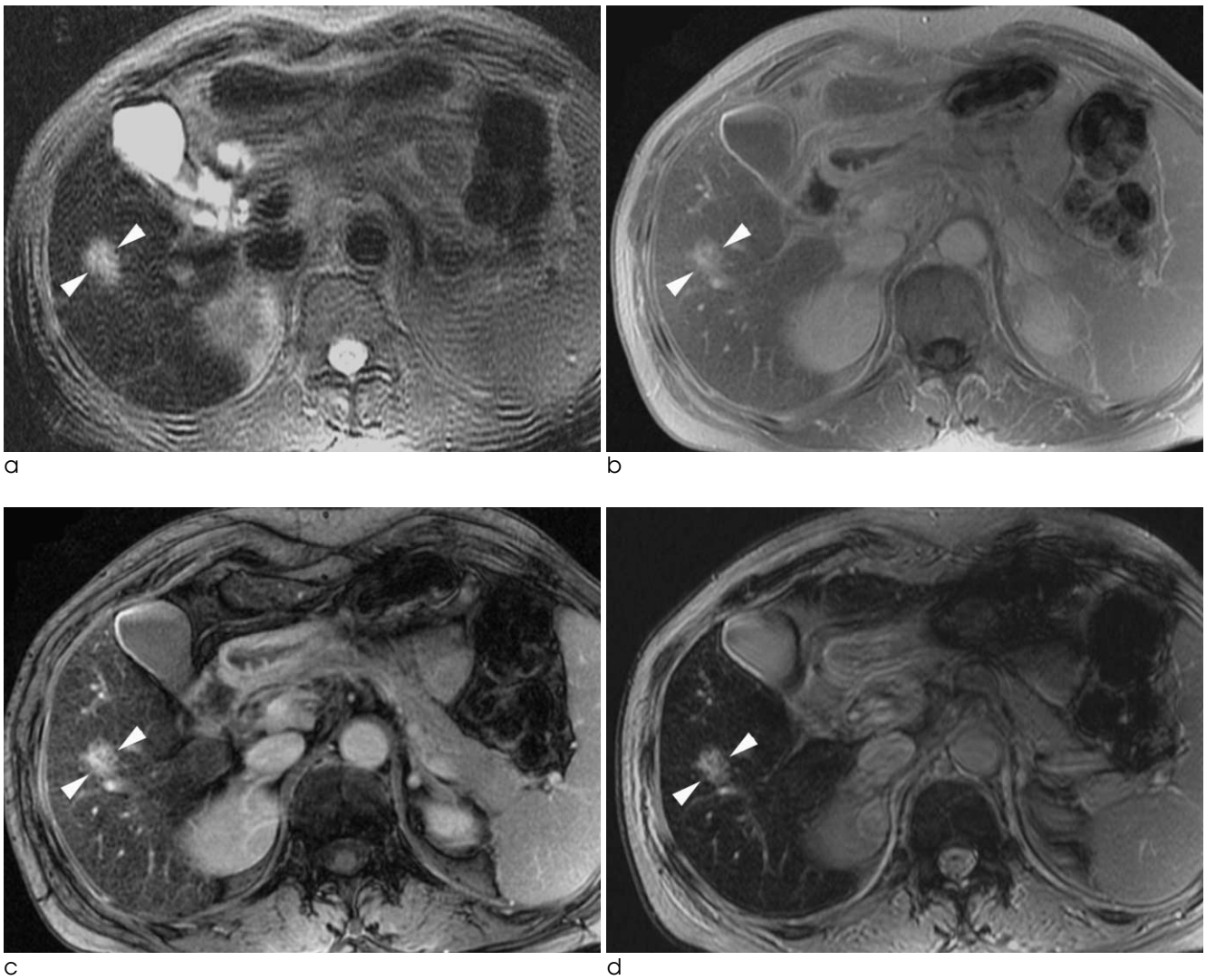

Fig. 3. A 51-year-old woman with a hepatic metastasis from uterine cervix cancer. After ferucarbotran injection, turbo spin-echo image (a) shows better lesion (arrowheads) conspicuity compared to gradient echo image with a TE of 2.4 msec (b) and comparable with gradient echo with a TE of 5.8 msec (c) and gradient echo with a TE of 10 msec (d).

higher than that at GRE_2.4 ($p < 0.001$). The mean CNRs of CCCs and metastases were higher than those of HCCs at GRE_10 ($p < 0.001$) and TSE ($p < 0.001$). However, the CNRs were comparable between GRE_2.4 ($p = 0.024$) and GRE_5.8 ($p = 0.004$) (Table 3).

Discussion

Compared to conventional 1.5T MRI unit, optimization of body imaging data acquisition using a 3T unit requires an appreciation of the changes in T1 and T2 (11). At higher field strength, T1 and T2 of normal tissues become lengthened and shortened, respectively (3, 11, 12); however, because of the various behaviors of relaxation times of a variety of different tissues, the optimal parameters that affect image contrast used in 3T imaging are still unknown (11). A definite helpful aspect of a 3T system is its higher SNR, but the benefit of high SNRs and CNRs would be partially cancelled out by the more prominent artifacts due to the susceptibility effects proportional to the magnetic field strength (4, 8, 13). However, the images obtained with a 3T system have been regarded as having comparable quality, allowing the assessment of focal liver lesions with equivalent confidence as the images acquired using 1.5T imaging (4, 6, 8, 11).

Additionally, SPIO particles that have accumulated in the Kupffer cells produce magnetic field heterogeneities in addition to the shortenings of T2 or T2*, which lead to signal loss or a decrease in the signal intensity of the liver (3, 14–16). Although there is no remarkable difference in the static imaging qualities between the 1.5T and 3T systems (6, 11), SPIO-enhanced imaging could be greatly influenced by an increased susceptibility effect. Regarding the scope of our present study, we assumed that the higher SNR on 3T SPIO-enhanced MRI can be attributed to the increased

Table 3. Quantitative Assessment of Lesion-to-liver Contrast-to-noise Ratios

MR Imaging pulse sequence	Lesion-to-liver CNR (Mean ± SD)			Comparison Between
	All Lesions (n = 170)	HCCs (n = 107)	CCCs and Metastases (n = 63)	HCC and Other Lesions (p)
TSE	10.1±7.7	8.2±5.6	13.6±9.6	< 0.001
GRE_2.4	6.3±6.4	5.4±5.7	7.9±7.3	0.024
GRE_5.8	12.1±9.1	10.2±6.9	15.5±11.4	0.004
GRE_10	19.8±14.4	16.4±11.7	25.7±16.9	< 0.001

CNR : Contrast to noise ratio
SD : Standard deviation
TSE : turbo spin echo
GRE_2.4 : gradient echo with TE of 2.4 msec
GRE_5.8 : gradient echo with TE of 5.8 msec
GRE_10 : gradient echo with TE of 10 msec

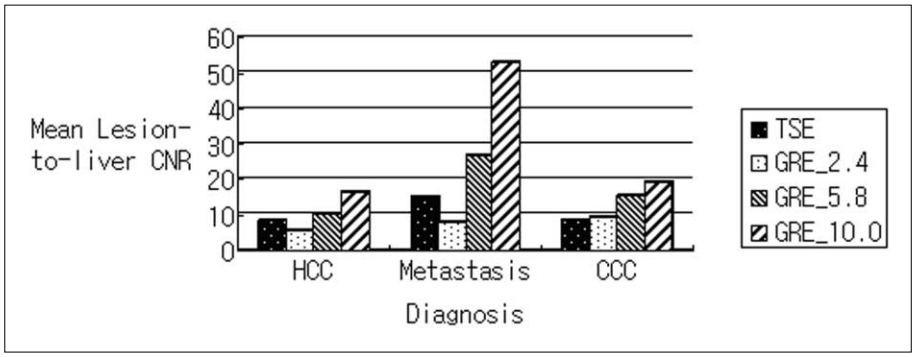

Fig. 4. Mean lesion-to-liver contrast-to-noise ratio (CNR) of hepatic lesions on four different fast MRI sequences after ferucarbotran injection. The y axis indicates the mean lesion-to-liver CNR.
TSE : turbo spin echo
GRE_2.4 : gradient echo with TE of 2.4 msec
GRE_5.8 : gradient echo with TE of 5.8 msec
GRE_10 : gradient echo with TE of 10 msec
HCC : Hepatocellular carcinoma
Mets : Metastasis
CCC : Cholangiocellular carcinoma

susceptibility of a 3T system to iron particles taken up by Kupffer cells in the liver parenchyma. Given that most hepatic tumors do not contain Kupffer cells, a greater signal loss of hepatic parenchyma on 3T would result in higher lesion-to-liver contrast accompanied by more pronounced artifacts from the adverse effects of increased susceptibility compared to those of 1.5T systems (4, 6).

Several studies have compared various imaging techniques using SPIO for the evaluation of liver tumors using either 1.5T or 3T MRI (2, 3, 4, 10, 17–23). Aside from T2-weighted imaging with a short TE similar to that of proton density imaging for maintaining the lesion signal intensity at a moderately higher degree, spoiled GRE with a long TE of about 10 msec provided a properly increased susceptibility effect of SPIO for optimized T2*-weighted imaging with a 1.5T system (10). In the present study using a 3T system, GRE_5.8 showed significantly better qualities in terms of hepatic contour, vascular landmarks and imaging artifacts compared to the remaining sequences including GRE_10, which has been regarded as an optimized sequence for the 1.5T system for SPIO-enhanced imaging. For GRE_10 on a 3T system, the accentuation of pulsation artifacts on the left lobe of the liver and the marginal blurring of anatomic landmarks resulting from a longer TE was more deteriorated with the negative effect of increased susceptibility artifacts from the higher field strength. Even though the mean CNR was higher on GRE_10 compared to those of the other sequences, the overall lesion conspicuity of GRE_5.8 was comparable with that of GRE_10 in the present study. Therefore, the results of the present study suggest that the overall value of GRE_5.8 is superior to that of GRE_10 for SPIO-enhanced imaging on a 3T system.

Because of the increased magnetization transfer effects and the reduced local field heterogeneities by the multiple 180° refocusing pulses, the effect of SPIO enhancement on signal loss in normal liver tissue is reduced in TSE images (18, 19, 24). In our present study, TSE was significantly inferior to all GRE sequences in the qualitative assessment. Lesion conspicuity and mean CNRs also showed pessimistic values with the TSE sequence. Even though it was beyond the scope of our study, the TSE sequence can help distinguish vessels from sub-centimeter lesions and may contribute to the approving consequences in the evaluation of focal liver lesions. The relatively low signal intensities of vascular structures in TSE sequences allow for improved conspicuity of small lesions (25).

Regarding the types of malignant focal lesions, the mean lesion-to-liver CNR of HCCs was lower than that of CCCs or metastases at all of the four SPIO-enhanced fast MRI sequences in the present study. In spite of the lack of information on our participants, we could speculate that the cirrhotic background of the liver for the HCC patients would disturb SPIO uptake in the background parenchyma, which might result in decreased CNR (26–28). Another possibility of the partial SPIO uptake in some well-differentiated HCCs might consequently decrease the lesion-to-liver CNR (29), which cannot occur in CCCs or metastases.

This study had several limitations. First, due to the retrospective manner of this study for the 1-cm or larger lesions for quantitative analysis, the true number of focal lesions could not be determined by a gold standard procedure. Therefore, the sensitivity and specificity of each sequence could not be calculated. Second, all of the images were obtained using 3T unit; direct comparison with images of 1.5T unit was not possible to differentiate the optimized breath-holding fast MR sequences based on the strength of the magnet. Due to the limited hardware performance of the early 3T unit used in this study, which was installed in 2002, the fast T2-weighted imaging sequence was not optimized for body imaging. The imaging quality of TSE has been improved during recent years with the 3T system, and the qualitative score of TSE would be different if the same study were to be performed with an updated system.

In conclusion, regarding overall quantitative and qualitative performances, GRE using a moderate echo time of 5.8 msec would provide most reliable data among the various fast breath-hold T2- or T2*-weighted imaging sequences for SPIO-enhanced hepatic MR imaging on the 3T unit despite the lower CNR compared to that of echo time of 10 msec attributable to fewer imaging artifacts and a comparable lesion conspicuity.

References

1. Van Beers BE, Gallez B, Pringot J. Contrast-enhanced MR iaging of the liver. Radiology 1997;203:297-306
2. Reimer P, Tombach B. Hepatic MRI with SPIO: detection and characterization of focal liver lesions. Eur Radiol 1998;8:1198-1204
3. von Falkenhausen M, Meyer C, Lutterbey G, et al. Intra-individual comparison of image contrast in SPIO-enhanced liver MRI at 1.5T and 3.0T. Eur Radiol 2007;17:1256-1261
4. Chang JM, Lee JM, Lee MW, et al. Superparamagnetic iron oxide-enhanced liver magnetic resonance imaging-comparison of 1.5T and 3.0T imaging for detection of focal malignant liver lesions. Invest Radiol 2006;41:168-174
5. Ramalho M, Altun E, Herédia V, Zapparoli M, Semelka R. Liver MR imaging: 1.5T versus 3T. Magn Reson Imaging Clin N Am 2007;15:321-347
6. von Falkenhausen MM, Lutterbey G, Morakkabati-Spitz N, et al. High-field-strength MR imaging of the liver at 3.0T: Intraindividual comparative study with MR imaging at 1.5T. Radiology 2006;241:156-166
7. Kim T, Murakami T, Hori M, Onishi H, Tomoda K, Nakamura H. Effect of superparamagnetic iron oxide on tumor-to-liver contrast at T2*-weighted gradient-echo MRI: comparison between 3.0T and 1.5T MR systems. J Magn Reson Imaging 2009;29:595-600
8. Nakada T. Clinical Experience on 3.0T systems in Niigata, 1996 to 2002. Invest Radiol 2003;38:377-384
9. Ward J, Guthrie JA, Wilson D, et al. Colorectal hepatic metastases: detection with SPIO-enhanced breath-hold MR imaging-comparison of optimized sequences. Radiology 2003;228:709-718
10. Kim MJ, Kim JH, Choi JY, et al. Optimal TE for SPIO-enhanced gradient-recalled echo MRI for the detection of focal hepatic lesions. AJR Am J Roentgenol 2006;187:W255-W266
11. de Bazelaire CM, Duhamel GD, Rofsky NM, Alsop DC. MR Imaging relaxation times of abdominal and pelvic tissues measured in vivo at 3.0T : preliminary results. Radiology 2004;230:652-659
12. Bottomley PA, Foster TH, Argersinger RE, Pfeifer LM. A review of normal tissue hydrogen NMR relaxation times and relaxation mechanisms from 1-100 MHz: dependence on tissue type, NMR frequency, temperature, species, excision, and age. Med Phys 1984;11:425-448
13. Zapparoli M, Semelka RC, Altun E, et al. 3.0-T MRI evaluation of patients with chronic liver diseases : initial observations. Magn Reson Imaging 2008;26:650-660
14. Hahn PF, Stark DD, Weissleder R, Elizondo G, Saini S, Ferrucci JT. Clinical application of superparamagnetic iron oxide to MR imaging of tissue perfusion in vascular liver tumors. Radiology 1990;174:361-366
15. Schneider G, Reimer P, Mabmann A, Kirchin MA, Morana G, Grazioli G. Contrast agents in abdominal imaging-current and future directions. Top Magn Reson Imaging 2005;16:107-124
16. Bellin MF, Zaim S, Auberton E, et al. Liver metastases: safety and Efficacy of detection with superparamagnetic iron oxide in MR imaging. Radiology 1994;193:657-663
17. Matsuo M, Kanematsu M, Itoh K, et al. Detection of malignant hepatic tumors with ferumoxides-enhanced MRI: Comparison of five gradient-recalled echo sequences with different TEs. AJR Am J Roentgenol 2004;182:235-242
18. Yoshikawa T, Mitchell DG, Hirota S, et al. Gradient- and spin-echo T2-weighted imaging for SPIO-enhanced detection and characterization of focal liver lesions. J Magn Reson Imaging 2006;23:712-719
19. Ward J, Chen F, Guthrie JA, et al. Hepatic lesion detection after superparamagnetic iron oxide enhancement: comparison of five T2-weighted sequences at 1.0 T by using alternative-free response receiver operating characteristic analysis. Radiology 2000;214:159-166
20. Kurokawa H, Togami I, Tsunoda M, Hiraki Y. Experimental study of fast and ultrafast T2-weighted imaging sequences using AMI-25 superparamagnetic iron oxide (SPIO). Acta Med Okayama 2001;55:41-50
21. Kumano S, Murakami T, Kim T, et al. Using superparamagnetic iron oxide-enhanced MRI to differentiate metastatic hepatic tumors and nonsolid benign lesions. AJR Am J Roentgenol 2003;181:1335-1339
22. Tanimoto A, Yuasa Y, Shinmoto H, et al. Superparamagnetic iron oxide-mediated hepatic signal intensity change in patients with and without cirrhosis: pulse sequence effects and Kupffer cell function. Radiology 2002;222:661-666
23. Kanematsu M, Itoh K, Matsuo M, et al. Malignant hepatic tumor detection with ferumoxides-enhanced MR imaging with a 1.5-T system: comparison of four imaging pulse sequences. J Magn Reson Imaging 2001;13:249-257
24. Elizondo G, Weissleder R, Stark DD, et al. Hepatic cirrhosis and hepatitis: MR imaging enhanced with superparamagnetic iron oxide. Radiology 1990;174:797-801
25. Zech CJ, Herrmann KA, Dietrich O, Horger W, Reiser MF, Schoenberg SO. Black-blood diffusion-weighted EPI acquisition of the liver with paraller imaging. Comparison with a standard T2-weighted sequence for detection of focal liver lesions. Invest Radiol 2008;43:261-266
26. Kuwatsuru R, Brasch RC, Muhler A, et al. Definition of liver tumors in the presence of diffuse liver disease: comparison of findings at MR imaging with positive and negative contrast agents. Radiology 1997;202:131-138
27. Tanimoto A, Yuasa Y, Shinmoto H, et al. Superparamagnetic iron oxide-mediated hepatic signal intensity change in patients with and without cirrhosis: pulse sequence and Kupffer cell function. Radiology 2002;222:661-666
28. Tanimoto A, Oshio K, Suematsu M, Pouliquen D, Stark DD. Relaxation effects of clustered particles. J Magn Reson Imaging 2001;14:72-77
29. Tang Y, Yamashita Y, Arakawa A, et al. Detection of hepatocellular carcinoma arising in cirrhotic livers: comparison of gadolinium and ferumoxides-enhanced MR imaging. AJR Am J Roentgenol 1999;172:1547-1554

대한자기공명의과학회지 14:31-40(2010)

간의 3T 자기공명영상에서 초상자성산화철 조영증강 급속호흡정지영상기법들간의 양적 및 질적 비교평가

[1]연세대학교 의과대학 강남세브란스병원 영상의학과

조경은 · 유정식 · 정재준 · 김주희 · 김기황

목적: 간의 국소병변에 대한 3T 자기공명영상에서 초상자성산화철 조영증강영상을 얻기 위한 여러 급속호흡정지대열들의 상대적 가치를 평가하고자 하였다.

대상 및 방법: 간의 자기공명영상을 시행하였던 환자들 중 한 개 이상의 악성 고형병소를 가진 102명의 연속으로 모은 환자들을 대상으로 초상자성산화철 조영제의 정맥주사 후 촬영한 3종류의 각각 다른 에코시간(2.4 msec〔GRE_2.4〕, 5.8 msec〔GRE_5.8〕, and 10 msec〔GRE_10〕)을 갖는 T2* 강조 경사에코영상들과 하나의 T2 강조 고속스핀에코영상(TSE)을 비교하였다. 두 명의 관찰자가 독립적으로 간의 윤곽, 혈관지표, 인공물, 병변의 명확도에 대해 각각 4점 스케일로 질적분석을 시행하였다. 양적분석을 위해 1 cm 이상의 크기를 갖는 170개의 병변들(간세포암 107개, 담도암 9개, 간전이암 54개)에 대하여 대조도잡음비를 측정하였다.

결과: GRE_5.8은 간윤곽, 혈관지표, 인공물에 대해 질적으로 가장 높은 점수를 받았으며($p < .001$) 간 병변의 명확도는 GRE_5.8과 GRE_10간에 유의한 차이가 없었다($p = .414$). 전체적으로 평균 대조도잡음비는 GRE_10(24.4±14.5), GRE_5.8(14.8±9.4), FSE(9.7±6.3), GRE_2.4(7.9±6.4)의 순으로 높았으며($p < .001$), 영상기법에 상관없이 담관암과 전이암의 평균 대조도잡음비가 간세포암에 비해 높았다($p < 0.05$).

결론: 3T 기기에서 악성 고형 간 병변의 진단을 위한 초상자성산화철 조영증강 급속 호흡정지기법들 중 5.8 msec의 중등도의 에코시간을 갖는 경사에코영상은 10 msec의 에코시간에 비해 대조도잡음비가 낮지만 전체적인 양적 및 질적 평가를 종합하여 볼 때 가장 우수한 영상을 제공할 수 있다.

통신저자 : 유정식, (135-720) 서울특별시 강남구 언주로 712번지, 강남세브란스병원 영상의학과
Tel. 82-2-2019-3510 Fax. 82-2-3462-5472 E-mail: yjsrad97@yuhs.ac